Energy & Environmental Science

COMMUNICATION

View Article Online
View Journal | View Issue

Cite this: *Energy Environ. Sci.*, 2015, **8**, 887

Received 12th November 2014
Accepted 14th January 2015

DOI: 10.1039/c4ee03596h

www.rsc.org/ees

β-cyclodextrin enhanced triboelectrification for self-powered phenol detection and electrochemical degradation†

Zhaoling Li,‡[ab] Jun Chen,‡[a] Jin Yang,‡[ac] Yuanjie Su,[a] Xing Fan,[a] Ying Wu,[a] Chongwen Yu[b] and Zhong Lin Wang*[ad]

We report a unique route that creatively harnessed β-cyclodextrin enhanced triboelectrification for self-powered phenol detection as well as electrochemical degradation. A detection sensitivity of 0.01 μM^{-1} was demonstrated in the sensing range of 10 μM to 100 μM. In addition, β-cyclodextrin enhanced triboelectrification was designed to harvest kinetic impact energy from wastewater waves to electrochemically degrade the phenol in a self-powered manner without using an external power source.

Broader context

As a common environmental disaster due to its high toxicity, considerable effort has been committed to remove phenol from the ambient environment, particularly from wastewater. Here, we report a unique route that creatively harnessed the β-cyclodextrin enhanced triboelectrification for self-powered phenol detection as well as electrochemical degradation. A detection sensitivity of 0.01 μM^{-1} was demonstrated in the sensing range of 10 μM to 100 μM. In addition, the β-cyclodextrin enhanced triboelectrification was designed to harvest kinetic impact energy from wastewater waves to electrochemically degrade the phenol in a self-powered manner without using an external power source. At a fixed wave velocity of 1.4 m s^{-1} and an initial phenol concentration of 80 mg L^{-1}, the generated power is capable of cleaning up to 90% of the phenol in the wastewater in 320 min. Given the compelling features, such as being self-powered, environmentally friendly, extremely cost-effective, simple, device reusable, high stability, high detection sensitivity and degradation efficiency, β-cyclodextrin enhanced triboelectrification renders an innovative approach for ambient phenol detection and electrochemical degradation.

Introduction

Phenol is corrosive to human eyes, skins, and the respiratory tract due to its high toxicity. Repeated or prolonged human contact with phenol may cause harmful effects on the liver, kidneys, heart and central nervous system, resulting in dysrhythmia, seizures and coma.[1] In almost all cases, phenol is damaging not only to individual species and populations, but also to natural biological communities.[2] Disturbingly, with plenty of discharging sources, such as chemical plants, pharmaceutical plants and petroleum refineries, phenol is one of the most serious and persistent organic pollutants that widely exists in the ambient environment, particularly in the surface waters.[3] Considerable effort has been committed to develop various techniques for phenol detection and degradation, including chromatographic,[4] spectrophotometric,[5] photocatalytic,[6] adsorptive,[7] and electrochemical analyses.[8] However, a wide adoption of these techniques may be shadowed by limitations such as sophisticated and expensive instruments, complex and time-consuming procedures, high energy consumption as well as high operating cost.[9,10]

Here, for the first time, we report a unique route that uses the energy harvested *via* β-cyclodextrin enhanced triboelectrification for a self-powered phenol treatment, which is an efficient integration of phenol detection and degradation. Relying on the β-cyclodextrin (β-CD) as the recognition element, the as-fabricated nanosensors can selectively capture and detect phenol molecules with a sensitivity of 0.01 μM^{-1} in a sensing range of 10–100 μM. The presented nanosenors are proved reusable after being refurbished with ethyl alcohol. Moreover, β-CD enhanced triboelectrification was creatively utilized to harvest the kinetic impact energy from wastewater waves, acting as a direct power source to electrochemically degrade phenol. Under a fixed wave velocity of 1.4 m s^{-1} and initial phenol concentration of 80 mg L^{-1}, the generated power was demonstrated to degrade 90% of the phenol in the wastewater in 320 min. The β-CD enhanced triboelectrification offers a unique

[a]*School of Materials Science and Engineering, Georgia Institute of Technology, Atlanta, Georgia 30332-0245, USA. E-mail: zlwang@gatech.edu*

[b]*Key Laboratory of Science & Technology of Eco-Textile, College of Textiles, Donghua University, Shanghai, 201620, China*

[c]*Department of Optoelectronic Engineering, Chongqing University, Chongqing, 400044, China*

[d]*Beijing Institute of Nanoenergy and Nanosystems, Chinese Academy of Sciences, Beijing, 100083, China*

† Electronic supplementary information (ESI) available. See DOI: 10.1039/c4ee03596h

‡ Authors with equal contribution.

route to treat the environmental phenol with a systematic integration of detection and degradation in a self-powered manner. With a collection of compelling features, such as high detection sensitivity and degradation efficiency, extremely low cost, simplicity and reusability, the presented work not only provides a new and efficient pathway for environmental chemical treatment, but also a solid "green" advancement in the fields of wastewater treatment, ecological sanitation, environmental degradation, monitoring, assessment and sustainability.

Results and discussion

The systematic phenol treatment using the β-CD enhanced triboelectrification consisted of two steps: detection and degradation. Regarding phenol detection, the as-fabricated nanosensor holds a multilayered structure with acrylic as supporting substrates, as schematically shown in Fig. 1a. On the upper substrate, a layer of polytetrafluoroethylene (PTFE) film was adhered acting as a contact surface with coated copper as the back electrode. On the lower substrate, a layer of Ti foil with surface grown TiO_2 nanowires is laminated as another contact surface. TiO_2 nanowires on the Ti foil were prepared *via* a coupling of the hydrothermal route in an alkali solution with an ion-exchange process.[11,12] A scanning electron microscopy (SEM) image of the grown TiO_2 nanowires on the titanium foil is presented in Fig. 1b with the measured average nanowire diameter and length of 73.4 nm and 1.92 μm, respectively. Furthermore, the corresponding X-ray diffraction (XRD) pattern of TiO_2 nanowires is shown in Fig. 1c. β-CD molecules were then assembled onto the TiO_2 nanowires as a surface chemical modification. Fig. 1d illustrates the charge transfer from the hydroxyl groups of β-CD to TiO_2 nanowires. Here, β-CD plays dual roles of a phenol recognition element and an electrical performance enhancer. A detailed description of the function of β-CD is presented in the following working principle section. An image of the as-fabricated phenol nanosensor is shown in Fig. 1e. The device has the dimensions of 4 cm × 4 cm. In addition, the detailed fabrication process is presented in the Experimental section.

Designed to use β-CD as the phenol recognition element as well as the electrical performance enhancer, the working principle of the devices based on β-CD enhanced triboelectrification can be elucidated in two aspects, namely, β-CD as surface chemical modification and triboelectrification for phenol detection and degradation. On one hand, β-CD is a cyclic oligosaccharide of seven α-D-glucose units connected through glycosidic α-1, 4 bonds, which are composed of hydrophobic internal cavity and hydrophilic external surface. This special molecular structure allows it to form a host/guest inclusion complex *via* various guest molecules with suitable polarity and dimension. The cavity diameter of β-CD has been found to be the most appropriate size for the selective adsorption of phenol,[13,14] which explains β-CD as a surface chemical modification for phenol recognition. On the other hand, the triboelectrification for phenol detection is a two-way coupling of the triboelectric effect and electrostatic induction.[15–22] At the original position, an initial contact of titanium dioxide with the

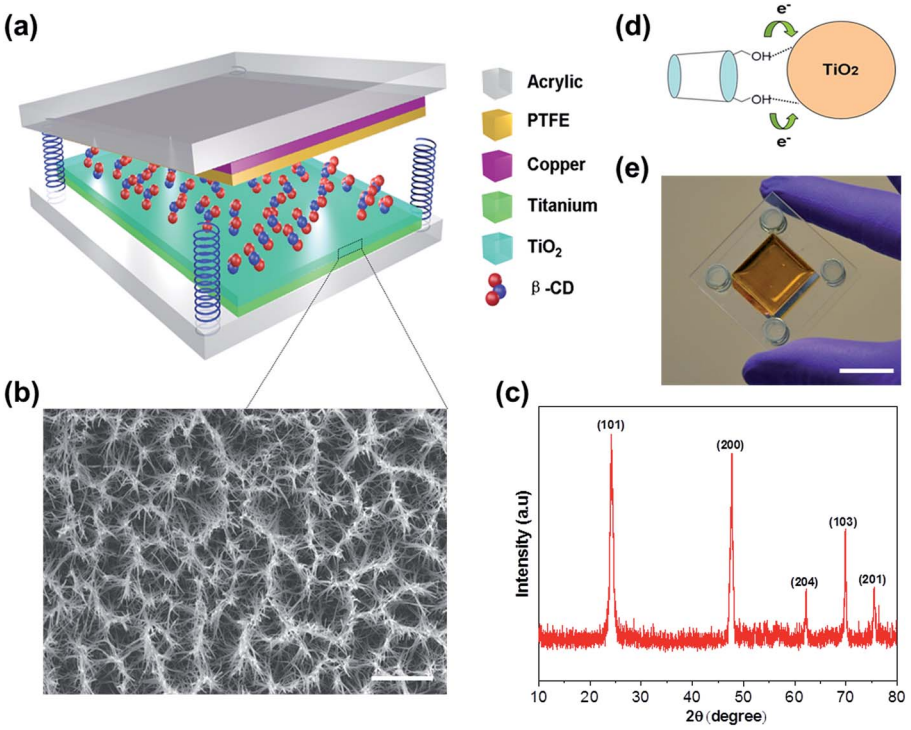

Fig. 1 (a) A sketch of the triboelectrification with β-cyclodextrin surface modification for phenol detection. (b) A SEM image of the TiO_2 nanowires. The scale bar is 5 μm. (c) The XRD spectra of the grown TiO_2 nanowires. (d) Schematic diagram for illustrating the charge transfer from the hydroxyl groups of β-cyclodextrin to TiO_2 nanowires. (e) An image of the as-fabricated device for phenol detection. The scale bar is 2 cm.

PTFE brought about charge transfer due to their different electron affinity, resulting in positive charges on the titanium dioxide and negative ones on the PTFE (Fig. S1a in ESI†). Once separation emerges, the induced electrical potential difference drives the electrons to flow from the Cu electrode to the Ti electrode (Fig. S1b in ESI†). By continuously increasing the separation, almost all the positive triboelectric charges are screened at the maximum separation (Fig. S1c in ESI†). As the two plates approach each other due to the spring elastic force, electrons are driven back from the Ti electrode to the Cu electrode (Fig. S1d in ESI†).[23–28] Given a consistent and cyclical operation of the two plates of the as-fabricated nanosensor at a fixed surface concentration of β-CD, the acquired output electrical signals in the external circuit are determined by the phenol concentration absorbed by the β-CD on the surface of the TiO_2 nanowires, which is the cornerstone of the β-CD enhanced triboelectrification for phenol detection. Furthermore, the electrical signals generated by the β-CD enhanced triboelectrification can also act as a direct power source to electrochemically degrade the phenol in the wastewater. Electricity is converted from the motion of wastewater waves, which renders a self-powered manner for phenol degradation.

In order to investigate the reasoning behind the β-CD functioning as an electrical performance enhancer, a series of electrical outputs was experimentally measured under various β-CD concentrations. The electric performance of the device was characterized in terms of the open-circuit voltage and the short-circuit current. The detailed working principle of the devices in both open-circuit and short-circuit conditions are depicted in Fig. S2 in ESI.† As demonstrated in Fig. 2a and b, both current and voltage signals were increasingly proportional to the surface concentrations of β-CD till a saturation point was reached, which was 80 μM by experimental observation. An output plateau emerged with a further increase in the concentrations beyond 80 μM. Fig. 2c and d present enlarged views of the current and voltage output signals at the β-CD concentration of 80 μM and a comparison with the output signals without β-CD surface modification. 6.0 times and 8.7 times enhancements of the current and voltage outputs were experimentally observed owing to the 80 μM β-CD surface modification. According to the triboelectric series (Fig. S3 in ESI†), a table showing the ability of a material to gain/lose electrons, PTFE is triboelectrically negative and has a large difference in the ability to attract and retain electrons as compared to TiO_2. Thus, when the two materials come in contact, PTFE grabs the electrons from TiO_2, whereas TiO_2 gives them up. Thus, PTFE is negatively charged and TiO_2 is positively charged, resulting in a potential drop between the two if they are separated. The enhancement in electrical output by β-CD modification is due to the charge transfer from β-CD to TiO_2. Namely, the binding of β-CD to the TiO_2 nanowire surface is ascribed to the adhesion of the hydroxyl groups, which derives from physical adsorption or H-bonding interactions. In addition, charge-transfer complex between the β-CD hydroxyl groups and the surface Ti atoms of the TiO_2 nanowires was formed owing to the coordination effect between the ligand and the metal under visible light irradiation.[29–33] Charge transfer from the hydroxyl groups of β-CD to TiO_2 nanowires arise from the new hybrid property of the TiO_2/β-CD complex. More surface charge transfer then takes place at the contact area upon the triboelectrification between PTFE and TiO_2. Consequently, β-CD is capable of acting as an effective chemical surface modifier, which can enhance triboelectrification and thus the device output performance.

After looking into the impact of β-CD concentrations on the electrical output, a further step was taken to evaluate the performance of β-CD enhanced triboelectrification for self-powered phenol detection. Under a fixed β-CD concentration of 80 μM, phenol solutions with various concentrations but constant volumes (20 μL) were dropped onto the surface of β-CD modified TiO_2 nanowires. Prior to further electrical measurement, the phenol treated nanosensors were dried at ambient temperature. The dependence of the positive peak values of the current and voltage outputs on the phenol concentrations are presented in Fig. 3a and b, respectively. In a certain phenol concentration region of 10–100 μM, both the current and voltage outputs are a monotonically decreasing function of phenol concentrations throughout the experimental time windows. The decrease is mainly attributed to a modified surface triboelectric behavior due to the adsorbed phenol molecules. The phenol will replace the position of TiO_2 to contact with PTFE. In comparison with TiO_2, phenol molecules have a lower tendency to transfer the electrons to PTFE, resulting in an electrical output that is dependent on the phenol concentrations. In order to render a direct view of the sensing performance of the β-CD enhanced triboelectrification for phenol detection, both the current ratio $((I_0 - I)/I_0)$ and the voltage ratio $((V_0 - V)/V_0)$ were plotted *versus* the phenol concentrations, as shown in Fig. 3c and d. These results reveal that the designed nanosensor is sensitive to the phenol molecules with a sensitivity of 0.01 μM^{-1} in the sensing range of 10–100 μM.

It is worth noting that triboelectric charges are also very dependent on the surface properties (*e.g.* roughness) of the two contacting surfaces. A control experiment was conducted to validate that the changes in triboelectric signals were mainly caused by the binding between β-CD and phenol. Different phenol solutions with various concentrations at a constant volume (20 μL) were directly dropped onto the TiO_2 surface without β-CD modification. As can be seen, increasing the concentration of phenol would increase the output of the as-fabricated device, as shown in Fig. S4 in ESI,† which was attributed to the surface roughness alteration due to the solid materials remaining on the TiO_2 surface after evaporation. However, such an effect seemed to be small and insignificant in comparison to the effect from β-CD surface modification, particularly when the phenol concentration was in a lower concentration range from 0 to 100 μM. This verified the dominant role of β-CD to alter triboelectric signals in the phenol detection processing.

Furthermore, control experiments were carried out to test the selectivity of the as-developed β-CD enhanced triboelectrification toward phenol detection as compared to other organic species. With a constant concentration of 50 μM for all the testing organic species, the obtained current ratio from the

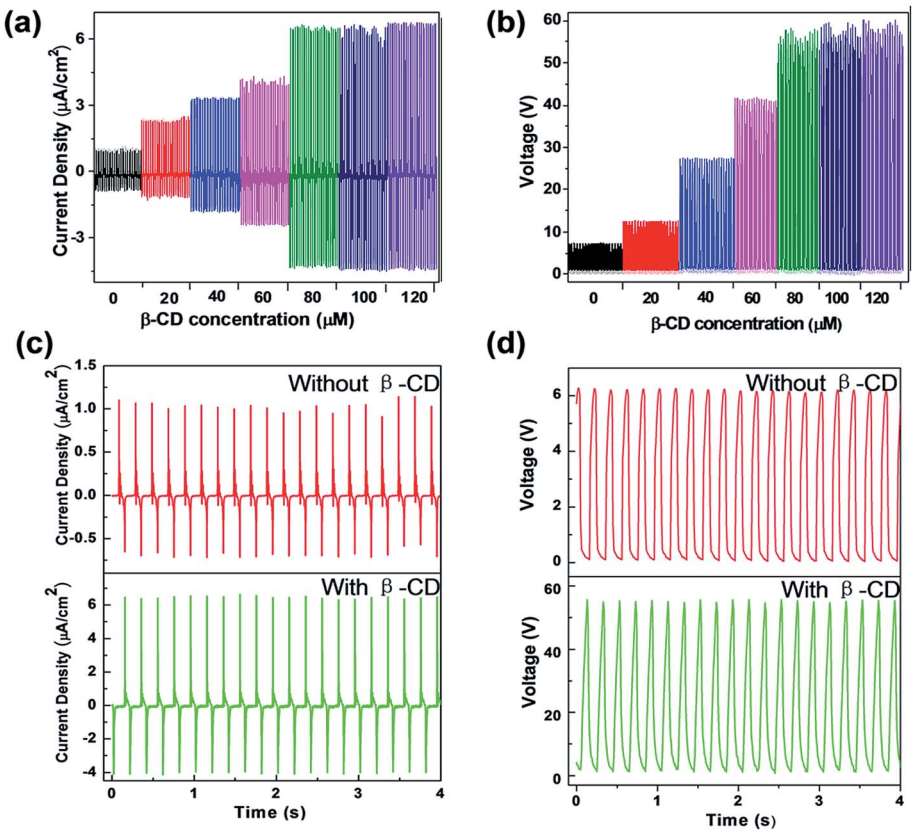

Fig. 2 (a) Dependence of the current output on the β-cyclodextrin concentrations. (b) Dependence of the voltage output on the β-cyclodextrin concentrations. A comparison of the measured current (c) and voltage (d) signals of the triboelectrification without and with an 80 μM β-cyclodextrin surface modification.

phenol absorbed nanosensor was far larger than that of the other organic species (Fig. 3e), which indicated that the β-CD enhanced triboelectrification is an effective means for phenol detection with excellent selectivity. In addition, besides the compelling features, such as high sensitivity, selectivity, extremely low cost, environmentally friendly and working in a self-powered manner, the β-CD enhanced triboelectrification based nanosensor is reusable and can be refurbished by ethyl alcohol rinsing after phenol detection. The measured current and voltage outputs of a refurbished nanosensor are demonstrated (Fig. S5 in ESI†), which show no observable output degradation after refurbishment. Furthermore, both the XRD pattern (Fig. 3f) and the SEM image (Fig. S6 in ESI†) show no chemical composition or surface morphology change after refurbishment, which proves the good reusability of the device for phenol detection.

Admittedly, the presence of water or environmental humidity is still a challenge to all the reported triboelectrification based energy harvesters or sensors because it largely affects the preservation of triboelectricity on the surfaces.[34–36] Experimentally, at the device level, the reported results indicated a negative impact on the output performance of the water. However, theoretically, at the fundamental level of the study of triboelectrification, the mechanism of contact electrification as well as the influence of humidity on it remains poorly understood. To date, the results of some studies have been proven inconclusive, suggesting that depending on humidity and the properties of contacting materials, the water contained in air can either promote or inhibit contact electrification.[37] Consequently, in this work, we harnessed a drying process to obviate the confusing situation.

We further investigated the stability of the devices. For the investigation, an electrodynamic shaker (from Labworks Inc.) that provides a sinusoidal wave was used as a vibration source with tunable frequency and amplitude. The experimental results are shown in Fig. 4. The current and voltage outputs of the device were measured and compared before and after a 50 000-cycle continuous operation. According to Fig. 4(a) and (b), the output only showed minor degradation. Furthermore, as shown in Fig. 4(c), the SEM images of the TiO_2 nanowires were taken after 10 000, 20 000, and 50 000 cycles of operation. It can be observed that the metallic oxide nanowires were almost unaffected by the continuous operation of the device, indicating the good durability of the device.

For a systematic treatment of ambient phenol, a further action was taken to degrade the phenol after it was detected. Here, a β-CD enhanced triboelectrification based energy harvester was developed as a power source to electrochemically degrade the phenol in the wastewater using the kinetic impact energy from water waves.[38–41] A schematic representation of the

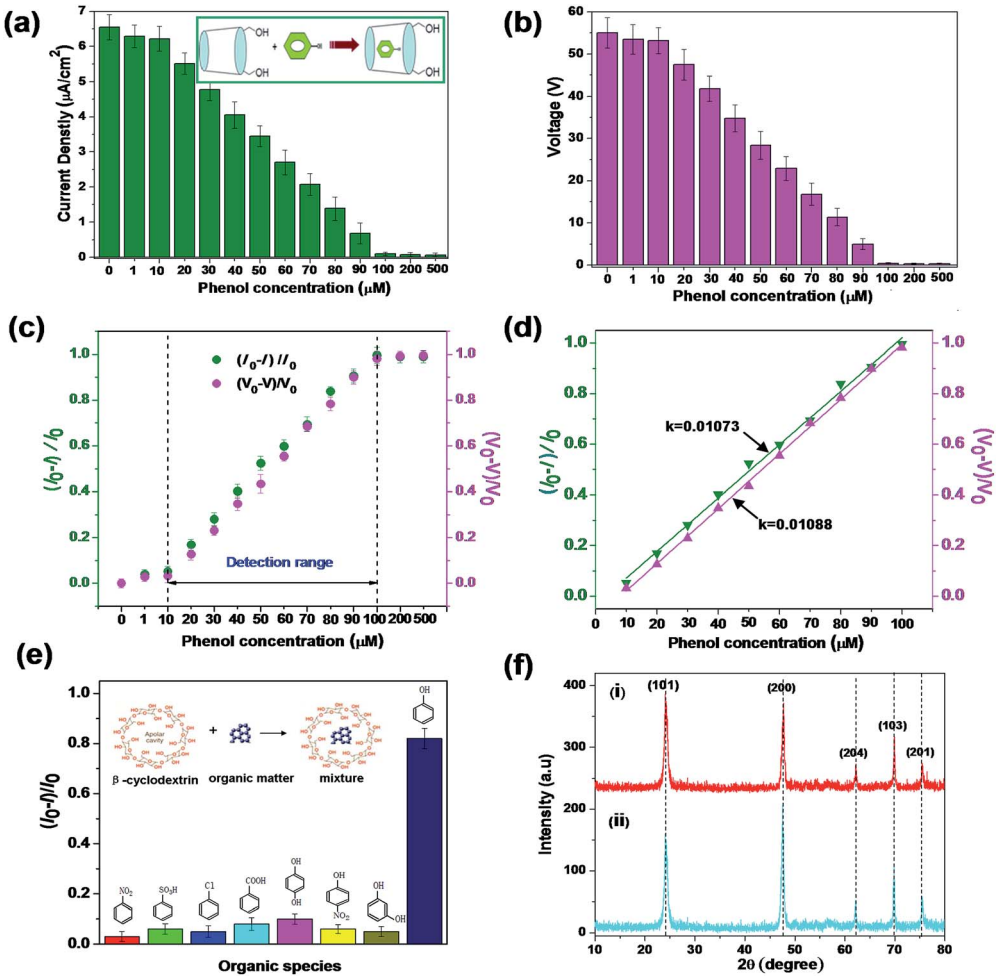

Fig. 3 Under a fixed 80 μM β-cyclodextrin surface modification, dependence of the current (a) and voltage (b) output on the phenol concentrations. Inset shows the reaction mechanism between β-cyclodextrin and a phenol molecule. (c) The sensitivity and detection range of the as-developed β-CD enhanced triboelectrification for phenol detection in terms of both current and voltage output. (d) A sensitivity of 0.01/μM was simultaneously achieved from both current and voltage signals with a detection range of 10–100 μM. (e) Selectivity of the as-developed β-CD enhanced triboelectrification for phenol detection. Inset shows an illustration of the reaction mechanism between β-cyclodextrin and different types of organic species. (f) A comparison of the XRD pattern of the TiO_2 nanowires: (i) as-grown and (ii) refurbished with 20 mL ethyl alcohol after phenol detection.

water wave energy harvester is shown in Fig. 5a, which has a multilayered structure with acrylic as supporting substrates. An annular ring shaped elastic rubber was employed to bridge the top plate of the "core" with the central-holed acrylic substrate, and thus it is capable of converting the water wave impact into the contact-separation of the two contact surfaces, PTFE and β-CD modified TiO_2 surfaces, and thus convert the wave energy into electricity as a sustainable power source for phenol degradation. Fig. 4b shows a close view of the "core" of the as-developed wave energy harvester. An image of the as-fabricated β-CD enhanced triboelectrification based wave energy harvester for phenol degradation is displayed (Fig. S7 in ESI†). An integrated self-powered phenol degradation system by harnessing wastewater wave energy is demonstrated in Fig. 5c. An as-fabricated wave energy harvester equipped with a Ti/PbO_2 anode and a Ti cathode was vertically fixed in a wastewater container. The detailed description of the wave energy harvester fabrication and the experimental setup for electrochemical phenol degradation are presented in the Experimental section.

With a surface concentration of 80 μM β-CD on the TiO_2 nanowires, a quantitative characterization of the output performance responding to various water wave velocities was systematically investigated. In order to quantitatively control the water waves, a linear motor was used to introduce a periodical impact onto the water. The water waves were propagated at different velocities by controlling the frequency and the impulse length of the linear motor. Furthermore, a directly proportional relationship was experimentally observed between the two, as shown in Fig. 5d and e. At a water wave velocity of 1.4 m s^{-1}, the generated current density and voltage are as high as 20 μA cm^{-2} and 70 V, respectively. The performance of the phenol degradation based on β-CD enhanced triboelectrification was evaluated at a fixed wave velocity of 1.4 m s^{-1}. Furthermore, the UV-visible absorption spectra of the phenol in

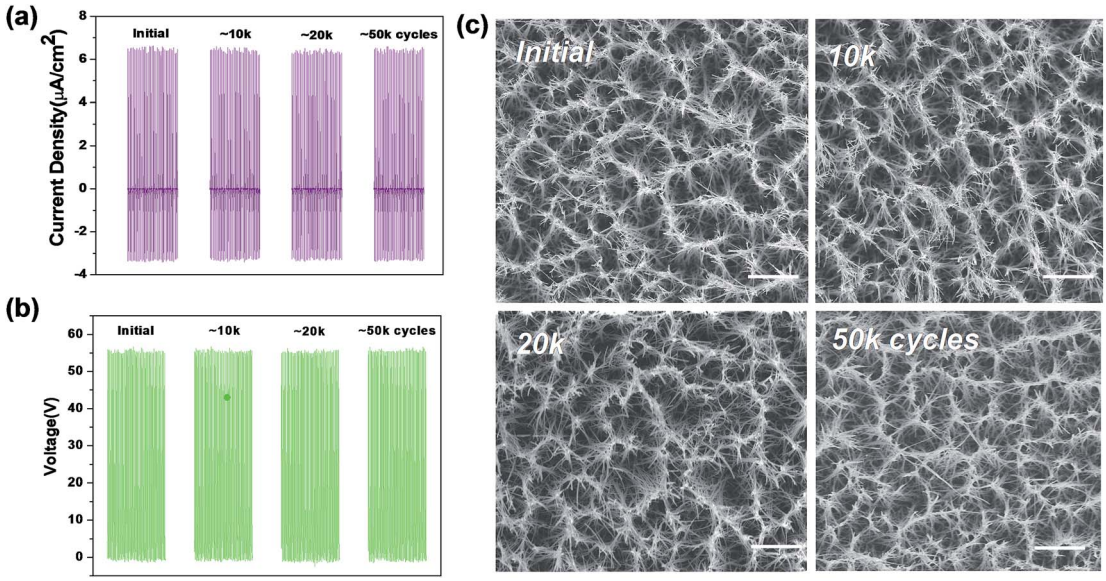

Fig. 4 Stability test of the as-fabricated devices. Current output (a), voltage output (b) of the device as well as the SEM images of the surface TiO_2 nanowires (c) after continuous working for up to 50 000 cycles. The scale bars are 5 μm.

the waste water, measured at fixed time intervals, are shown in Fig. 6a. With increasing in electrochemical degradation time, the characteristic absorption peak intensity of phenol in the wastewater decreases evidently, indicating the effectiveness of the route for self-powered phenol degradation. The inset of Fig. 6a shows the calibration curve of phenol concentration at the wavelength of 269 nm, which is the wavelength corresponding to the characteristic absorption peaks. In order to further validate that the decrease in the phenol absorption peak intensity is attributed to the electrochemical degradation, a control experiment was conducted without triboelectrification or external power sources. The UV-visible curve of the phenol

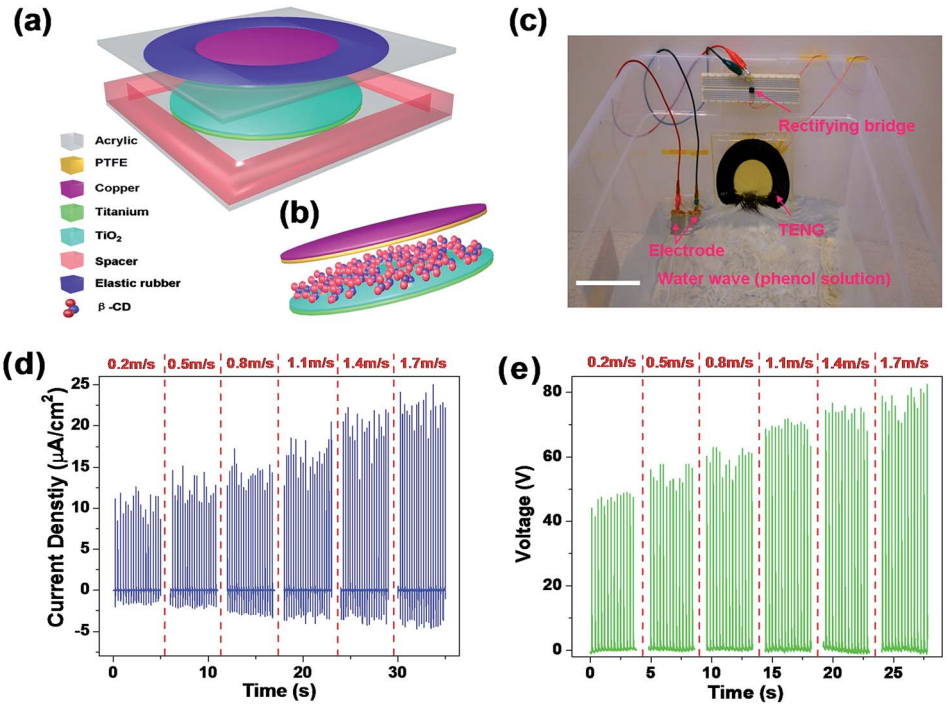

Fig. 5 (a) Structural design of the β-CD enhanced triboelectrification for self-powered phenol degradation using kinetic impact energy from water waves. (b) An illustration of the core part of the β-CD enhanced triboelectrification for phenol degradation. (c) Demonstration of an integrated self-powered phenol degradation system by harnessing water waves. The scale bar is 15 cm. The dependence of the current (d) and voltage (e) output of the β-CD enhanced triboelectrification on the wave velocities.

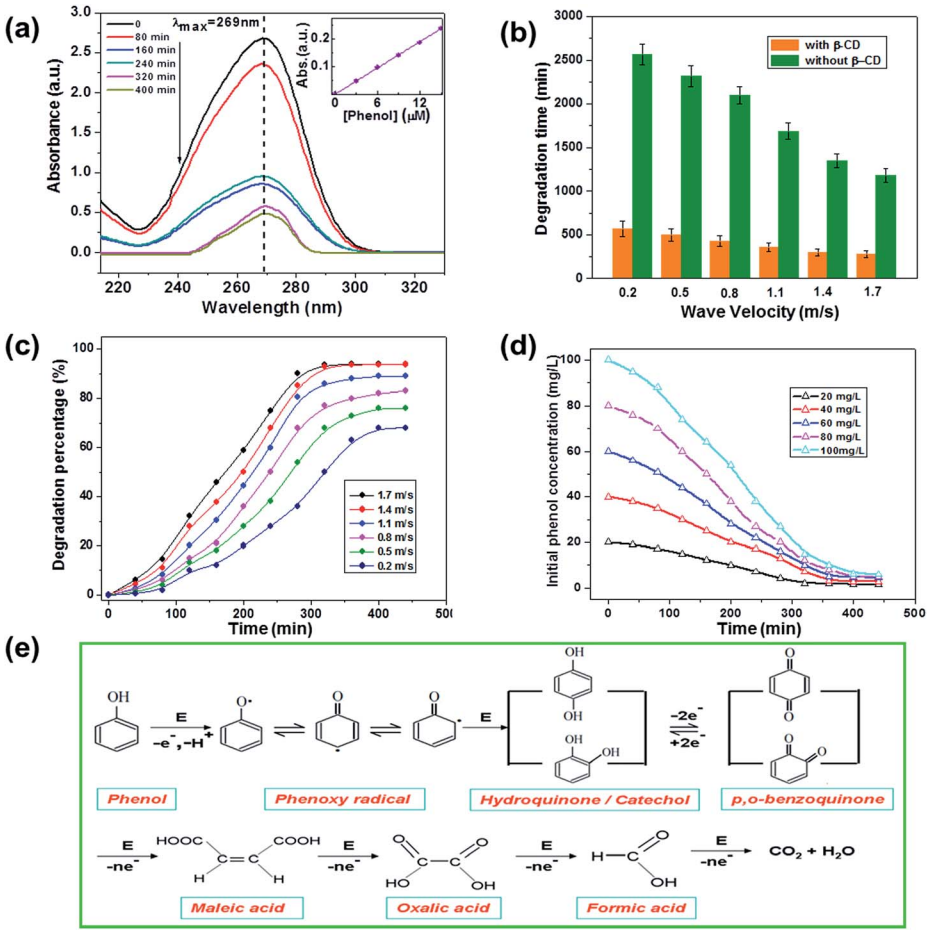

Fig. 6 (a) UV-visible absorption spectra of the phenol in the wasted water with increasing electrochemical degradation time by the β-CD enhanced triboelectrification. Inset shows the calibration curve of the phenol concentration from the absorption spectra at a wavelength of 269 nm. (b) Comparison of the phenol degradation time *versus* the water wave velocity when the degradation percentage reaches 90%, without and with an 80 μM β-cyclodextrin surface modification. (c) Comparison of the phenol degradation percentage *versus* the degradation time under different propagating speeds of water waves. (d) Comparison of the initial phenol concentration *versus* the degradation time under fixed water wave velocity of 1.4 m s^{-1}. (e) The proposed reaction mechanisms of the phenol electrochemical degradation.

solution remained unchanged as the time passed by (Fig. S8 in ESI†). Electricity is a must for the electrochemical degradation of phenol. Without electricity, phenol cannot degrade on its own over time.

Factors, particularly the β-CD surface modification, wave velocity and the phenol initial concentration, can significantly influence the effectiveness of the proposed routes for phenol electrochemical degradation. A systematic investigation of these three factors was made to comprehensively evaluate the performance of the β-CD enhanced triboelectrification based self-powered phenol degradation. First, the influence of β-CD surface modification on the degradation performance was studied *via* a comparison of the time needed for reaching a phenol degradation percentage of 90% under various wave velocities at a fixed initial phenol concentration of 80 mg L^{-1}. Technically, in an electrochemical degradation processing, the degradation efficiency is proportional to the applied power. As shown in Fig. 6b, without β-CD surface modification, phenol still degrades over time, but the degradation efficiency is very low due to a relatively smaller electrical output of the devices. However, after surface modification with β-CD, the β-CD enhanced triboelectrification, which contributes to a larger electrical output of the devices, significantly boosts the speed of phenol electrochemical degradation and decreases the time required for completely mineralizing the phenol in the wastewater.

Secondly, as an important factor for the electrical output, the influence of water wave velocity on the degradation performance was also studied at a fixed initial phenol concentration of 80 mg L^{-1}. As demonstrated in Fig. 6c, to reach the same phenol degradation percentage, a shorter time is needed with a larger wave velocity. Similarly, given a fixed degradation time interval, a larger wave velocity will contribute to a larger phenol degradation percentage in the wastewater. Specifically, given a wave velocity of 1.4 m s^{-1}, the degradation percentage of phenol in the wastewater is up to 90% in 320 min. Furthermore, in the beginning, the phenol concentration in wastewater is high. The amount of phenol that can be degraded per unit time is more,

which corresponds to a higher degradation rate. As the degradation reaction proceeds, the phenol concentration in wastewater continues to decrease. This inevitably leads to a low degradation efficiency. Hence, the degradation rate increases at first (before 320 min) and then remains constant over time.

In addition, the initial phenol concentration in the wastewater is another factor that needs to be explored for a systematic evaluation of the degradation performance. It is observed from Fig. 6d that under a fixed wave velocity of 1.4 m s^{-1}, more time is required for the electrochemical degradation starting with a higher initial phenol concentration. Moreover, though the initial phenol concentration varies, the residual content of phenol remains almost the same after a continuous degradation for 360 min. Furthermore, it is encouraging to find that the electrochemical degradation process is more effective at higher initial phenol concentrations, which renders the proposed route very practical and promising for industrial wastewater treatment.

Experimentally, the phenol electrochemical degradation initiated at the Ti/PbO_2 anode electrode, where the color of the solution changed from the initial colorless to yellow (40–260 min), and lastly to colorless (300 min) (Fig. S9 in ESI†). The proposed reaction mechanisms of the phenol electrochemical degradation are illustrated in Fig. 6e. In the electrochemical oxidation process, the phenol pollutants can not only be mineralized by the hydroxyl radicals produced on the anode surface, but can also be directly oxidized and degraded on the surface of the anodes. Phenol was first transformed into the phenoxy radical, and then, the hydroxyl radicals produced on the anode surface attacked the benzene rings to produce hydroquinone and catechol. The hydroquinone and catechol were further degraded to benzoquinone, which turned the solution from colorless to yellow.[8–10] Subsequently, the ring was broken, and the benzoquinone was degraded into various carboxylic acids such as maleic acid, oxalic acid and formic acid. Finally, these organic acid intermediates were mineralized into CO_2 and H_2O, and thus, the solution became colorless again.

Conclusions

In summary, we demonstrate a unique route that creatively harnessed the β-CD enhanced triboelectrification for both self-powered phenol detection and electrochemical degradation. Relying on the β-CD as the recognition element, the as-fabricated nanosensors can selectively capture and detect the phenol molecules in an ambient environment. A detection sensitivity of 0.01 μM^{-1} was experimentally read by calibrating both the current and the voltage signals in a sensing range of 10–100 μM. The presented nanosenors are proved reusable after being refurbished with ethyl alcohol. In addition, the β-cyclodextrin enhanced triboelectrification was designed to harvest kinetic impact energy from water waves to electrochemically degrade the phenol in a self-powered manner without supplying an external power. At a fixed wave velocity of 1.4 m s^{-1} and initial phenol concentration of 80 mg L^{-1}, the generated power is capable of cleaning up to 90% of the phenol in the wastewater in 320 min. The justified concept of self-powered phenol treatment using triboelectrification is a green alternative to traditional methods, which could arouse a broad range of audience, particularly from the fields of wastewater treatment, ecological sanitation, environmental degradation, monitoring, assessment and sustainability. Furthermore, it can not only be applied to the ambient phenol detection and degradation, but also can be extended to other common organic pollutants in the wastewater, such as methylbenzene, benzaldehyde, chlorobenzene, aniline, and benzoic acid, which is promising and could possible change the current method of wastewater treatment.

Experimental section

Growth of TiO_2 nanowires on Ti foils

Ti foils with the dimensions of 2 cm × 2 cm were ultrasonically and ordinarily cleaned in acetone, ethanol, and water for 10 min. Subsequently, the treated Ti foils were put into an NaOH aqueous solution (1 M, 20 mL) in a 25 mL Teflon-lined stainless steel autoclave. Then, the sealed autoclaves were placed in ovens at the temperatures of 220 °C for 24 h and then cooled to room temperature. After the hydrothermal reaction, Ti foils were covered with $Na_2Ti_2O_4(OH)_2$ nanowires, which were immersed into HCl solutions (1 M, 20 mL) for 10 min after being washed by DI water. In this processing, Na^+ was replaced with H^+, forming $H_2Ti_2O_4(OH)_2$ nanowires on the Ti foils. Then, the Ti foils were dried at room temperature after they were removed from the HCl solution and washed with DI water again. TiO_2 nanowires on the Ti foils were obtained after a heat treatment of the samples in an oven at 500 °C for 3 h.

Surface modification of TiO_2 nanowires with β-CD

A physical adsorption method[42–44] was used to assemble a layer of β-CD molecules onto the TiO_2 nanowires. TiO_2 nanowires on the Ti substrate were immersed into the β-CD solutions with different concentrations at room temperature for 12 h. Subsequently, the β-CD modified TiO_2 surface was thoroughly washed with ethanol and acetone to remove the excess of β-CD molecules and then dried under vacuum.

Fabrication of a nanosensor for phenol detection

Two pieces of acrylic with the dimensions of 4 cm × 4 cm were shaped by laser cutting as supporting substrates. Four holes were drilled at each corner for spring installation. A layer of Cu (50 nm) was deposited onto the PTFE thin film (25 μm) by physical vapor deposition (PVD), which was then laminated onto the inner surface of the acrylic substrate as the top plate with Cu as the back electrode. The Ti/TiO_2 composite was assembled onto the bottom acrylic substrate with TiO_2 nanowires facing the PTFE on the top plate. Finally, conducting wires were connected to the Ti and Cu electrodes for subsequent electrical measurements.

Fabrication of a wave energy harvester for phenol degradation

Two pieces of different acrylic, square-shaped and central-holed, were shaped by laser cutting as supporting substrates

with the dimensions of 15 cm × 15 cm. A layer of Cu (50 nm) was deposited onto the PTFE thin film (25 μm) by PVD. Then, the Cu/PTFE composite was laminated onto the inner surface of the acrylic substrate as the top plate. The Ti/TiO_2 composite was assembled on the bottom acrylic substrate with TiO_2 nanowires facing the PTFE on the top plate. An annular ring shaped elastic rubber was employed to bridge the top plate of the wave energy harvester with the central-holed acrylic substrate. Finally, conducting wires were connected to the Ti and Cu electrodes for the subsequent electrochemical degradation of phenol.

Characterization

A Hitachi SU8010 field emission scanning electron microscope, operated at 5 kV and 10 mA, was used to measure the size and shape of the grown TiO_2 nanowires. A PANalytical X'Pert PRO diffractometer (Almelo, Netherlands) with Cu Kα radiation (λ = 0.15418 nm) was employed to measure the X-ray diffraction (XRD) patterns of the as-prepared TiO_2 nanowires. The electrical signals were acquired using a programmable electrometer (Keithley Model 6514) and a low-noise current preamplifier (Stanford Research System Model SR570).

Electrochemical degradation of phenol solution

The electrochemical degradation of phenol was performed in a plastic box filled with 2000 mL of phenol solution at room temperature. Prior to degradation, 0.1 g of NaCl as the electrolyte was added into solution to improve the conductivity of the phenol solution. Due to good chemical stability and high electrocatalytic activity, the Ti and Ti/PbO_2 electrodes were placed into the phenol solution and acted as the cathode and the anode, respectively. A rectifying bridge was connected to the wave energy harvester to convert the alternating current to direct current signals. The absorbance spectra of the phenol solution was monitored and measured at fixed time intervals using an UV-visible spectrophotometer (JASCO V-630).

Acknowledgements

The research was supported by U.S. Department of Energy, Office of Basic Energy Sciences, Division of Materials Sciences and Engineering under Award DE-FG02-07ER46394, the Hightower Chair foundation, and the "thousands talents" program for pioneer researcher and his innovation team, China, the National Natural Science Foundation of China (Grant no. 51432005), Beijing City Committee of science and technology (Z131100006013004, Z131100006013005).

Notes and references

1 M. A. Warner and J. V. Harper, *Anesthesiology*, 1985, **62**, 366–367.
2 J. Sołoducho and J. Cabaj, *J. Biomater. Nanobiotechnol.*, 2013, **4**, 17–27.
3 J. Wang, J. Lu, S. Y. Ly, B. Tian, W. K. Adeniyi and R. A. Armendariz, *Anal. Chem.*, 2000, **72**, 2659–2663.
4 T. Zhao, J. He, X. Wang, B. Ma, X. Wang, L. Zhang, P. Li, N. Liu, J. Lu and X. Zhang, *J. Pharm. Biomed. Anal.*, 2014, **98**, 311–320.
5 X. X. Han, L. Chen, U. Kuhlmann, C. Schulz, I. M. Weidinger and P. Hildebrandt, *Angew. Chem., Int. Ed.*, 2014, **53**, 2481–2484.
6 M. Mukthar Ali and K. Y. Sandhya, *Carbon*, 2014, **70**, 249–257.
7 W. Ma, J. Li, X. Tao, J. He, Y. Xu, J. C. Yu and J. Zhao, *Angew. Chem., Int. Ed.*, 2003, **42**, 1029–1032.
8 H. Li, Y. Chen, Y. Zhang, W. Han, X. Sun, J. Li and L. Wang, *J. Electroanal. Chem.*, 2013, **689**, 193–200.
9 W. Ma, Z. Cheng, Z. Gao, R. Wang, B. Wang and Q. Sun, *Chem. Eng. J.*, 2014, **241**, 167–174.
10 G. Chen, *Sep. Purif. Technol.*, 2004, **38**, 11–41.
11 Z.-H. Lin, Y. Xie, Y. Yang, S. Wang, G. Zhu and Z. L. Wang, *ACS Nano*, 2013, **7**, 4554–4560.
12 J.-Y. Liao, B.-X. Lei, H.-Y. Chen, D.-B. Kuang and C.-Y. Su, *Energy Environ. Sci.*, 2012, **5**, 5750–5757.
13 X. Chen, X. Cheng and J. J. Gooding, *Anal. Chem.*, 2012, **84**, 8557–8563.
14 J. Feng, A. Miedaner, P. Ahrenkiel, M. E. Himmel, C. Curtis and D. Ginley, *J. Am. Chem. Soc.*, 2005, **127**, 14968–14969.
15 G. Zhu, J. Chen, T. Zhang, Q. Jing and Z. L. Wang, *Nat. Commun.*, 2014, **5**, 3426.
16 W. Yang, J. Chen, G. Zhu, J. Yang, P. Bai, Y. Su, Q. Jing and Z. L. Wang, *ACS Nano*, 2013, **7**, 11317–11324.
17 J. Yang, J. Chen, Y. Yang, H. Zhang, W. Yang, P. Bai, Y. Su and Z. L. Wang, *Adv. Energy Mater.*, 2014, **4**, 1301322.
18 G. Zhu, P. Bai, J. Chen and Z. L. Wang, *Nano Energy*, 2013, **2**, 688–692.
19 Y. Suzuki, *IEEJ Trans. Electr. Electron. Eng.*, 2011, **6**, 101–111.
20 G. Zhu, J. Chen, Y. Liu, P. Bai, Y. Zhou, Q. Jing, C. Pan and Z. L. Wang, *Nano Lett.*, 2013, **13**, 2282–2289.
21 H. W. Lo and Y. C. Tai, *J. Micromech. Microeng.*, 2008, **18**, 104006–104013.
22 R. Tashiro, N. Kabei, K. Katayama and E. Tsuboi, *J. Artif. Organs*, 2002, **5**, 239–245.
23 J. Yang, J. Chen, Y. Liu, W. Yang, Y. Su and Z. L. Wang, *ACS Nano*, 2014, **8**, 2649–2657.
24 P. D. Mitcheson, P. Miao, B. H. Stark, E. M. Yeatman, A. S. Holmes and T. C. Green, *Sens. Actuators, A*, 2004, **115**, 523–529.
25 Z.-H. Lin, G. Zhu, Y. S. Zhou, Y. Yang, P. Bai, J. Chen and Z. L. Wang, *Angew. Chem., Int. Ed.*, 2013, **52**, 1–6.
26 J. Boland, Y. H. Chao, Y. Suzuki and Y. C. Tai, *Micro Electro Mechanical Systmes, IEEE The Sixteenth Annual International Conference*, 2003, pp. 538–541.
27 Y. Suzuki, D. Miki, M. Edamoto and M. Honzumi, *J. Micromech. Microeng.*, 2010, **20**, 104002.
28 J. Chen, G. Zhu, W. Yang, Q. Jing, P. Bai, Y. Yang, T. C. Hou and Z. L. Wang, *Adv. Mater.*, 2013, **25**, 6094–6099.
29 T. Wu, G. Liu and J. Zhao, *J. Phys. Chem. B*, 1998, **102**, 5845–5851.
30 J. Zhao, T. Wu, K. Wu, K. Oikawa, H. Hidaka and N. Serpone, *Environ. Sci. Technol.*, 1998, **32**, 2394–2400.

31 T. Rajh, L. X. Chen, K. Lukas, T. Liu, M. C. Thurnauer and D. M. Tiede, *J. Phys. Chem. B*, 2002, **106**, 10543–10552.
32 S. Kim and W. Choi, *J. Phys. Chem. B*, 2005, **109**, 5143–5149.
33 Y. Zhou and M. Antonietti, *J. Am. Chem. Soc.*, 2003, **125**, 14960–14961.
34 H. Zhang, Y. Yang, Y. Su, J. Chen, C. Hu, Z. Wu, Y. Liu, C. P. Wong, Y. Bando and Z. L. Wang, *Nano Energy*, 2013, **2**, 693–701.
35 H. Guo, J. Chen, L. Tian, Q. Leng, Y. Xi and C. Hu, *ACS Appl. Mater. Interfaces*, 2014, **6**, 17184–17189.
36 V. Nguyen and R. Yang, *Nano Energy*, 2013, **2**, 604–608.
37 H. T. Baytekin, B. Baytekin, S. Soh and B. A. Grzybowski, *Angew. Chem., Int. Ed.*, 2011, **50**, 6766–6770.
38 Z.-H. Lin, G. Cheng, L. Lin, S. Lee and Z. L. Wang, *Angew. Chem., Int. Ed.*, 2013, **52**, 12545–12549.
39 J. Scruggs and P. Jacob, *Science*, 2009, **323**, 1776–1779.
40 G. Zhu, Y. Su, P. Bai, J. Chen, Q. Jing, W. Yang and Z. L. Wang, *ACS Nano*, 2014, **8**, 6031–6037.
41 Y. Su, X. Wen, G. Zhu, J. Yang, J. Chen, P. Bai, Z. Wu, Y. Jiang and Z. L. Wang, *Nano Energy*, 2014, **9**, 186–195.
42 X. Zhang, X. Li and N. Deng, *Ind. Eng. Chem. Res.*, 2012, **51**, 704–709.
43 J. M. Notestein, E. Iglesia and A. Katz, *J. Am. Chem. Soc.*, 2004, **126**, 16478–16486.
44 H. Choi, S. O. Kang, J. Ko, G. Gao, H. S. Kang, M.-S. Kang, M. K. Nazeeruddin and M. Gratzel, *Angew. Chem., Int. Ed.*, 2009, **48**, 5938–5941.

